Chemical Physics Letters 644 (2016) 62–67

Contents lists available at ScienceDirect

Chemical Physics Letters

journal homepage: www.elsevier.com/locate/cplett

Effect of reverse intersystem crossing rate to suppress efficiency roll-off in organic light-emitting diodes with thermally activated delayed fluorescence emitters

Munetomo Inoue[a,b,1], Tomas Serevičius[b,c,1], Hajime Nakanotani[a,b,d,e], Kou Yoshida[a,b], Toshinori Matsushima[b,d], Saulius Juršėnas[c], Chihaya Adachi[a,b,d,e,*]

[a] Department of Applied Chemistry, 744 Motooka, Nishi, Fukuoka 819-0395, Japan
[b] Center for Organic Photonics and Electronics Research, Kyushu University, 744 Motooka, Nishi, Fukuoka 819-0395, Japan
[c] Institute of Applied Research, Vilnius University, Saulėtekio 9-III, LT-10222 Vilnius, Lithuania
[d] Japan Science and Technology Agency (JST), ERATO, Adachi Molecular Exciton Engineering Project, 744 Motooka, Nishi, Fukuoka 819-0395, Japan
[e] International Institute for Carbon Neutral Energy Research, Kyushu University, 744 Motooka, Nishi, Fukuoka 819-0395, Japan

ARTICLE INFO

Article history:
Received 7 September 2015
In final form 25 November 2015
Available online 8 December 2015

ABSTRACT

Electroluminescence efficiency roll-off in organic light-emitting diodes with thermally activated delayed fluorescence emitters 1,2-bis(carbazol-9-yl)-4,5-dicyanobenzene (2CzPN) and 3-(9,9-dimethylacridin-10(9H)-yl)-9H-xanthen-9-one (ACRXTN) is investigated by considering intramolecular exciton relaxation processes. Electroluminescence efficiency roll-off at high current density is dramatically suppressed using ACRXTN as an emitter instead of 2CzPN because of suppressed bimolecular exciton annihilation processes such as singlet–triplet and triplet–triplet annihilation. The rate constant of reverse intersystem crossing from triplet to singlet excited states of ACRXTN is about 300 times higher than that of 2CzPN, decreasing triplet exciton density and suppressing exciton annihilation processes under optical and electrical excitation.

1. Introduction

Because organic light-emitting diodes (OLEDs) can exhibit nearly 100% internal electroluminescence (EL) quantum efficiency (η_{int}), they are attractive for next-generation lighting sources as well as display applications. Although nearly 100% η_{int} has been achieved, the decrease of EL efficiency, known as roll-off, at high brightness [1] is a serious problem limiting the development of high-brightness OLEDs. Over the past two decades, two types of organic luminescent compounds have mainly been developed as emitters for OLEDs. OLEDs using fluorescent materials as emitters exhibit rather weak roll-off characteristics, although their η_{int} is intrinsically limited to 25% because only 25% of excitons, corresponding to singlet excitons, could be harvested under electrical excitation [1,2]. In contrast, although efficient room-temperature phosphorescent materials such as tris(2-phenylpyridinato)iridium(III) ($Ir(ppy)_3$) can provide nearly 100% η_{int}, the large accumulation of triplet excitons in an emitter layer causes considerable bimolecular deactivation, *i.e.*, triplet–triplet annihilation (TTA), because of the rather long lifetimes of triplet excitons (a few μs) compared with those of typical singlet excitons (a few ns) [1–5]. In fact, according to reported simulations [1,4,6], the efficiency roll-off of OLEDs using (E)-2-(2-(4-(dimethylamino)styryl)-6-methyl-4H-pyran-4-ylidene)malononitrile as a fluorescent emitter and $Ir(ppy)_3$ as a phosphorescent emitter has been ascribed to mainly singlet–triplet annihilation (STA) [1,6] and TTA [1,4], respectively.

Recently, we proposed a unique triplet harvesting process in OLEDs, namely thermally activated delayed fluorescence (TADF) [7–9]. In OLEDs using TADF molecules as an emitter (TADF–OLEDs), although a maximum η_{int} of nearly 100% has been achieved, they also exhibit substantial roll-off behavior similar to that of phosphorescence-based OLEDs [8–10]. To understand the origin of the roll-off of TADF–OLEDs, here we investigate the exciton annihilation processes in OLEDs containing the sky-blue TADF molecules 1,2-bis(carbazol-9-yl)-4,5-dicyanobenzene (2CzPN) and 3-(9,9-dimethylacridin-10(9H)-yl)-9H-xanthen-9-one (ACRXTN), and reveal that both STA and TTA contribute to the roll-off of

* Corresponding author at: Center for Organic Photonics and Electronics Research (OPERA), 744 Motooka, Nishi, Fukuoka 819-0395, Japan.
E-mail address: adachi@cstf.kyushu-u.ac.jp (C. Adachi).
[1] These authors contributed equally to this work.

http://dx.doi.org/10.1016/j.cplett.2015.11.042
0009-2614/

Table 1
Summary of $\eta_{EQE,\,max}$, J_0, η_{EQE} at 1000 cd m^{-2}, k_{STA}, and k_{TTA} of OLEDs containing 2CzPN and ACRXTN as emitters.

TADF materials	$\eta_{EQE,\,max}$ [%]	J_0 [mA cm^{-2}]	η_{EQE} at 1000 cd m^{-2} [%]	k_{STA} [10^{-11} cm^3 s^{-1}]	k_{TTA} [10^{-15} cm^3 s^{-1}]
2CzPN	10.3	1.6	2.2	2.1	5.0
ACRXTN	12.1	104	11.0	1.9	5.1

TADF–OLEDs. We demonstrate that the rate constant of reverse intersystem crossing (RISC) from triplet to singlet excited states (k_{RISC}) of ACRXTN (k_{RISC} = ~10^5 s^{-1}) is about 300 times higher than that of 2CzPN (k_{RISC} = ~10^3 s^{-1}), and this larger k_{RISC} of ACRXTN decreases the triplet exciton density, suppressing STA and TTA under electrical excitation.

2. Experimental

The molecular structures of TADF emitters 2CzPN and ACRXTN are shown in Figure 1a. OLEDs containing 2CzPN and ACRXTN as emitters were fabricated by conventional vacuum deposition on glass substrates coated with a 100-nm-thick indium tin oxide (ITO) layer under a base pressure of around 7×10^{-4} Pa. The OLEDs possessed the structure glass substrate/ITO (100 nm)/α-NPD (30 nm)/mCP (10 nm)/5 mol% 2CzPN- or ACRXTN-doped mCP (15 nm)/PPT (10 nm)/TPBi (40 nm)/LiF (0.8 nm)/Al (100 nm), where α-NPD, mCP, PPT and TPBi are 4,4′-bis[*N*-(1-naphthyl)-*N*-phenyl-amino]biphenyl, *N*,*N*′-dicarbazolyl-3,5-benzene, 2,8-bis(diphenylphosphoryl)dibenzo-[b,d]thiophene, and 2,2′,2″-(1,3,5-benzenetriyl)tris[1-phenyl-1H-benzimidazole], respectively. Current density (*J*)–voltage (*V*)–external quantum efficiency (η_{EQE}) characteristics and EL spectra of the OLEDs were measured using an integrating sphere connected to a source meter (2400, Keithley Instruments) and a photonic multichannel analyzer (PMA-12, Hamamatsu Photonics). For optical measurements, 100-nm-thick mCP films doped with 5 mol% 2CzPN or ACRXTN were fabricated on quartz substrates by vacuum deposition. Photoluminescence (PL) spectra and PL quantum yields (PLQYs) of these films were measured by a spectrofluorometer (FluoroMax-4, Horiba Jobin Yvon) and PLQY measurement system (C9920-02, Hamamatsu Photonics), respectively. PL lifetimes of the films were measured under vacuum using a streak camera (C4334, Hamamatsu Photonics), and a nitrogen gas laser (MNL200, Lasertechnik) with an excitation wavelength of 337 nm and pulse width of 500 ps as an excitation source. The rate constants shown in Figure 1b were calculated from the values of PLQY and PL lifetime as previously reported [10]. The transient EL response of the OLEDs during long pulse voltage excitation was also measured using a photomultiplier tube (C9525-02, Hamamatsu Photonics) and pulse generator (WF 1974, NF corporation). The pulse width was 500 μs and the repetition frequency was 0.5 Hz for this measurement.

Table 2
Summary of *J*, η_{EQE}, and $\eta_{EQE}/\eta_{EQE,\,max}$ of OLEDs containing 2CzPN and ACRXTN at different N_T.

TADF materials	N_T [10^{17} cm^{-3}]	*J* [mA cm^{-2}]	η_{EQE} [%]	$\eta_{EQE}/\eta_{EQE,\,max}$
2CzPN	1.0	0.1	8.7	0.84
	5.0	0.6	6.6	0.64
	10.0	1.8	4.8	0.47
ACRXTN	1.0	7.8	10.3	0.85
	5.0	51.0	7.7	0.64
	10.0	100	6.0	0.49

3. Results and discussion

PL and EL spectra, and *J*–*V* and η_{EQE}–*J* characteristics of the OLEDs with 2CzPN and ACRXTN are presented in Figure 2. The maximum η_{EQE} ($\eta_{EQE,\,max}$), current density when η_{EQE} decreases to half of the initial η_{EQE} (J_0), η_{EQE} at 1000 cd m^{-2}, rate constant of STA (k_{STA}), and rate constant of TTA (k_{TTA}) are summarized in Table 1. These

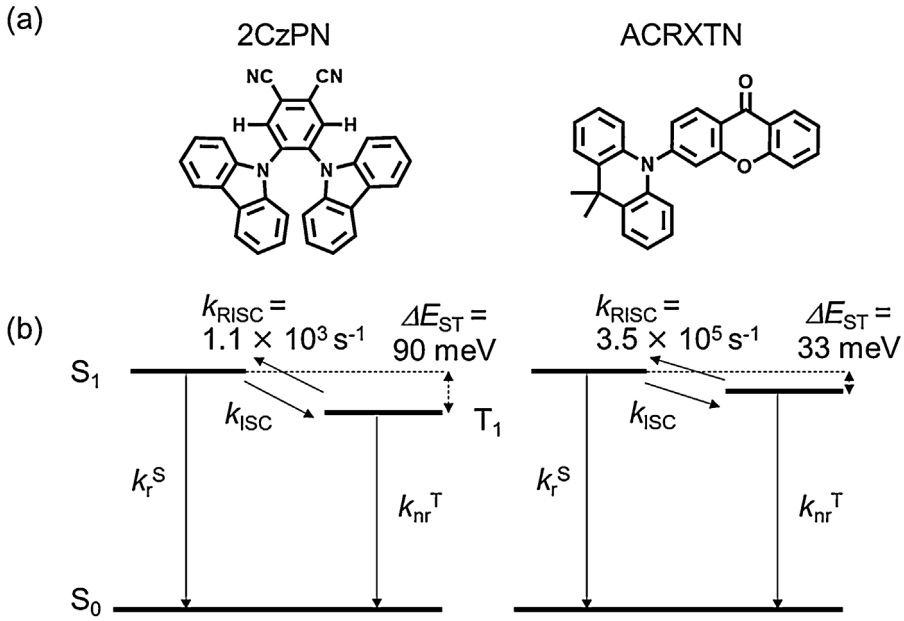

Figure 1. (a) Molecular structures of 2CzPN and ACRXTN and (b) illustration of intramolecular relaxation processes of TADF materials. The rate constants of each intramolecular relaxation process are summarized in Table 3.